COMPUTER METHODS IN MATERIALS SCIENCE
Informatyka w Technologii Materiałów

Publishing House
A K A P I T

Vol. 19, 2019, No. 2

ON THE EXTRAPOLATED VMS-POD METHOD FOR INCOMPRESSIBLE FLOWS[1]

FATMA G. EROGLU[1]*, SONGUL KAYA[2]

[1]Department of Mathematics, Faculty of Science, Bartın University, 74110, Bartın, Turkey
[2]Department of Mathematics, Middle East Technical University, 06531 Ankara, Turkey
[*]Corresponding author: fguler@bartin.edu.tr

Abstract

In this study, proper orthogonal decomposition based reduced-order modelling and variational multiscale stabilization method are utilized for the incompressible Navier-Stokes equations. Also, the difficulties resulting from nonlinearity are eliminated by using the extrapolation. Theoretical analysis of the method is presented. To check the efficiency of the proposed method, we utilize the test problem of 2D channel flow past a cylinder.

Key words: Proper orthogonal decomposition, Extrapolated Crank-Nicholson, Reduced-order modelling, Projection-based variational multiscale, Finite Element Method

1. INTRODUCTION

The incompressible Navier-Stokes equations (NSE) in dimensionless form are given as:

$$\begin{aligned} \mathbf{u}_t - \nu\Delta u + (\mathbf{u}\cdot\nabla)\mathbf{u} + \nabla p &= \mathbf{f} \text{ in } (0,\tau]\times\Omega \\ \nabla\cdot\mathbf{u} &= 0 \text{ in } (0,\tau]\times\Omega \\ \mathbf{u} &= \mathbf{0} \text{ in } (0,\tau]\times\partial\Omega \\ \mathbf{u}(0,\mathbf{x}) &= \mathbf{u}_0 \text{ in } \Omega \end{aligned} \tag{1}$$

where $\mathbf{u}(t;\mathbf{x})$, $p(t,\mathbf{x})$ are the fluid velocity, the pressure fields, respectively.

Let $\Omega\subset\mathbb{R}^d$; $d\in\{2,3\}$ be a confined porous enclosure with polygonal boundary $\partial\Omega$. The initial velocity field is given as $\mathbf{u}_0$. The parameter in (1) is the kinematic viscosity $\nu > 0$, inversely proportional to Reynolds number Re.

The main challenges in solving NSE are due to the complex behaviour of the flow at high Re and the absence of the analytical solution. Also, when full order methods are used to find a numerical solution of (1), large number of degrees of freedom cause large algebraic systems and high computational costs. As a remedy, we utilize Galerkin based reduced-order modelling with proper orthogonal decomposition (POD).

The POD method has been found useful to get a low-dimensional system (Kunisch & Volkwein, 2001; Xia et al., 2013; San & Borggaard, 2015; Kalugin & Strijhak, 2016). It captures the dominant energetic modes from an ensemble of data, which are assumed to acquire by using standard Galerkin finite element procedure. POD uses the obtained modes to represent snapshots. Naturally, POD reduces the complexity of the problem. This yields a remarkable reduction in computational cost and the number of degrees of freedom. However, due to the use of POD in the nonlinear problem, numerical instability appears. To address this issue, we use the variational multiscale (VMS) stabilization technique. In the VMS method, the large scales are defined by using projections and, artificial viscosity is added only to small scales (John & Kaya, 2008; John et al., 2006). In that

[1]The paper presented during YIC 2019, ECCOMAS Young Investigators Conference held in Kraków, Poland on September 1-6, 2019

ISSN 1641-8581

way, it destroys small eddies. As the basic functions of POD are in descending order, it is easy to decompose the scales, i.e. large and small scales are sorted naturally in the POD method. The VMS-POD combination has been found efficient for many multiphysics problems such as convection-diffusion-reaction equations (Iliescu & Wang, 2013), Oseen equations (Roop, 2013), Navier stokes equations (Eroglu et al., 2017; Iliescu & Wang, 2014), Darcy Brinkman equations (Eroglu et al., 2019a; Eroglu et al., 2019b).

In this paper, we consider a method based on Crank-Nicholson temporal discretization. Besides, to conserve accuracy of the scheme, we also utilize the extrapolation with Crank-Nicholson to the nonlinear terms at each time step.

This paper is planned as follows. In Section 2, we introduce the continuous and discrete variational formulation of (1), then we establish an extrapolated VMS-POD formulation of the scheme. In Section 3, we prove stability and convergence analysis. Two numerical experiments are given in Section 4. Finally, we present the conclusions in Section 5.

2. FULL ORDER MODEL FOR THE NSE SYSTEM

Throughout this paper, the standard Sobolev spaces and their norms are used. The notations $\|\cdot\|_k$ $\|\cdot\|_{L^p}$ and $\|\cdot\|$ will show the norm in $\left(H^k(\Omega)\right)^d$ spaces, $\left(L^p(\Omega)\right)^d$ Lebesgue spaces $(1\le p<\infty,\ p\ne 2)$ and the usual $L^2(\Omega)$ space respectively. $(\cdot,\cdot)$ denote inner product in the $L^2(\Omega)$ space. The continuous velocity, pressure spaces and divergence free space of velocity are given as:

$$\begin{aligned}&\mathbf{X}:=\left(\mathbf{H}_0^1(\Omega)\right)^d, Q:=L_0^2(\Omega)\\&\mathbf{V}:=\left\{\mathbf{v}\in\mathbf{X}:(\nabla\cdot\mathbf{v},q)=0,\forall q\in Q\right\}\end{aligned}\tag{2}$$

Note that, $\mathbf{H}^{-1}$ is a dual space of $\mathbf{X}$ with dual norm:

$$\|\mathbf{f}\|_{-1}=\sup_{\mathbf{v}\in X}\frac{|(\mathbf{f},\mathbf{v})|}{\|\nabla\mathbf{v}\|}\tag{3}$$

The discrete norms are defined as:

$$\||v|\|_{k,p}:=\left(\Delta t\sum_{n=1}^{M}\|v^n\|_p^k\right)^{1/k},\quad \||v|\|_{\infty,p}:=\max_{0\le n\le M}\|v^n\|_p,\tag{4}$$

The continuous weak formulation of (1) reads as follows: Find $\mathbf{u}$: $(0,\tau]\to\mathbf{X}$, p: $(0,\tau]\to Q$, satisfying:

$$\begin{aligned}&(\mathbf{u}_t,\mathbf{v})+\nu(\nabla\mathbf{u},\nabla\mathbf{v})+b(\mathbf{u},\mathbf{u},\mathbf{v})-(p,\nabla\cdot\mathbf{v})=(\mathbf{f},\mathbf{v})\\&(q,\nabla\cdot\mathbf{u})=0\end{aligned}\tag{5}$$

for all $(\mathbf{v},q)\in(\mathbf{X},Q)$, where:

$$b(\mathbf{u},\mathbf{v},\mathbf{w}):=\frac{1}{2}\left(\left((\mathbf{u}\cdot\nabla)\mathbf{v},\mathbf{w}\right)-\left((\mathbf{u}\cdot\nabla)\mathbf{w},\mathbf{v}\right)\right)\tag{6}$$

represent the skew-symmetric form of the convective term.

A conforming finite element method is considered for (5) such that Th is a triangulation with mesh size h. The finite element spaces $\mathbf{X}_h\subset\mathbf{X}$, $Q_h\subset Q$ satisfy the discrete inf-sup condition. Moreover, $\mathbf{X}_h$, Q_h are composed of piecewise polynomials of degree at most k and $k-1$, respectively. These spaces satisfy the following approximation properties:

$$\begin{aligned}&\inf_{w_h\in\mathbf{X}_h}\left\{\|\mathbf{u}-w_h\|^2\right\}\le Ch^{2k+2}\|\mathbf{u}\|_{k+1}^2\\&\inf_{w\in\mathbf{X}_h}\left\{\|\nabla(\mathbf{u}-w_h)\|^2\right\}\le Ch^{2k}\|\mathbf{u}\|_{k+1}^2\\&\inf_{q_h\in Q_h}\left\{\|p-w_h\|^2\right\}\le Ch^{2k}\|p\|_k^2\end{aligned}\tag{7}$$

where $\mathbf{u}\in\mathbf{H}^{k+1}$.

The discretely divergence free space is given by:

$$\mathbf{V}_h=\left\{\mathbf{v}_h\in\mathbf{X}_h:(\nabla\cdot\mathbf{v}_h,q_h)=0,\forall q_h\in Q_h\right\}\tag{8}$$

As $\mathbf{V}_h$ is a closed subspace of $\mathbf{X}_h$, the approximation properties (7) are valid for the following $\mathbf{V}_h$ formulation: Find $\mathbf{u}_h\in\mathbf{V}_h$ satisfying:

$$(\mathbf{u}_{h,t},\mathbf{v}_h)+\nu(\nabla\mathbf{u}_h,\nabla\mathbf{v}_h)+b(\mathbf{u}_h,\mathbf{u}_h,\mathbf{v}_h)=(\mathbf{f},\mathbf{v}_h)\tag{9}$$

for all $\mathbf{v}_h\in\mathbf{V}_h$.

We now formulate POD for the system (9). Let $C=\mathrm{span}\left\{\mathbf{u}(\cdot,t_1),\mathbf{u}(\cdot,t_2),\ldots,\mathbf{u}(\cdot,t_M)\right\}$ be an ensemble of snapshots for given time instances $t_j=j\Delta t$, $j=1,\ldots,M$, for $M=\tau/\Delta t$. In the aim of finding low dimensional POD basis functions ξ_1, $\xi_2\ldots\xi_r$, we solve the error minimization problem of:

$$\arg\min_{\xi_1,\xi_2,\cdot,\xi_r}\frac{1}{M}\sum_{k=1}^{M}\left\|\mathbf{u}(\cdot,t_k)-\sum_{j=1}^{r}\left(\mathbf{u}(\cdot,t_k),\xi_j(\cdot)\right)\xi_j(\cdot)\right\|^2\tag{10}$$

such that $(\xi_i,\xi_j)=\delta_{ij}$, $1\le i,j\le r$, $r<<d$, and $d=\mathrm{rank}(C)$. When the equation (10) is modified, it turns into an eigenvalue problem as:

$$A\gamma=\lambda\gamma\tag{11}$$

where $A\in\mathbb{R}^{M\times M}$ with $A_{ki}=\frac{1}{M}\left(\mathbf{u}(\cdot,t_i),u(\cdot,t_k)\right)$, $i,k=1,\ldots,M$ is the snapshots correlation matrix. The solution of eigenvalue problem (11) becomes:

$$\xi_j(\cdot)=\frac{1}{\sqrt{\lambda_j}}\sum_{k=1}^{M}\left(\gamma_j\right)_k\mathbf{u}\left(\cdot,t_k\right),\quad 1\le j\le r \tag{12}$$

where λ_m, γ_m denote the eigenvalue and the eigenvector of A. Also, the error estimation satisfies (see (Kunisch & Volkwein, 2001), for detailed derivation):

$$\frac{1}{M}\sum_{k=1}^{M}\left\|\mathbf{u}\left(\cdot,t_k\right)-\sum_{j=1}^{r}\left(\mathbf{u}\left(\cdot,t_k\right),\xi_j(\cdot)\right)\xi_j(\cdot)\right\|^2=\sum_{j=r+1}^{d}\lambda_i \tag{13}$$

As the all eigenvalues are sorted in descending order, the basis functions $\{\xi_i\}_{i=1}^{r}$ correspond to the first r largest eigenvalues $\{\lambda_i\}_{i=1}^{r}$, respectively. For the projection-based VMS-POD formulation, we need the following spaces:

$$\mathbf{X}_r=span\{\xi_1,\xi_2,\ldots,\xi_r\} \tag{14}$$

$$\mathbf{X}_R=span\{\xi_1,\xi_2,\ldots,\xi_R\} \tag{15}$$

$$L_{R,\mathbf{u}}=\nabla\mathbf{X}_R \tag{16}$$

Note that we have $\mathbf{X}_R\subseteq\mathbf{X}_r\subset\mathbf{V}_h\subset\mathbf{X}$. The L^2 projection operators $\mathcal{P}_r:L^2\to\mathbf{X}_r$, $\mathcal{P}_R:L^2\to L_{R,\mathbf{u}}$ are defined by:

$$\left(\mathbf{u}-\mathcal{P}_r\mathbf{u},\mathbf{v}_r\right)=0,\quad\forall\mathbf{v}_r\in X_r \tag{17}$$

$$\left(\mathbf{u}-\mathcal{P}_R\mathbf{u},\mathbf{v}_r\right)=0,\quad\forall\mathbf{v}_R\in L_{R,\mathbf{u}} \tag{18}$$

To bind the POD projection error, we need the following lemma.

Lemma 2.1. *For true solution* $\mathbf{u}^n$ *at time* ^{tn}, *we have*:

$$\frac{1}{M}\sum_{n=1}^{M}\left\|\mathbf{u}^n-\mathcal{P}_r\mathbf{u}^n\right\|^2\le C\left(h^{2k+2}\|\mathbf{u}\|_{2,k+1}^2+\sum_{i=r+1}^{d}\lambda_i\right) \tag{19}$$

$$\frac{1}{M}\sum_{n=1}^{M}\left\|\nabla\left(\mathbf{u}^n-\mathcal{P}_r\mathbf{u}^n\right)\right\|^2\le C\left(\left(h^{2k}+\|S_r\|_2 h^{2k+2}\right)\|\mathbf{u}\|_{2,k+1}^2+\zeta_r^2\right) \tag{20}$$

Where $\zeta_r=\sqrt{\sum_{i=r+1}^{d}\|\xi_i\|_1^2\lambda_i}$ *and* S_r *denots the POD stiffness matrices with* $\left(S_r\right)_{ij}=\int_\Omega\nabla\xi_i\cdot\nabla\xi_j d\mathbf{x}$

Proof. For the proof see (Iliescu & Wang, 2014).

We also assume that the following inequalities hold:

$$\left\|\mathbf{u}^n-\mathcal{P}_r\mathbf{u}^n\right\|^2\le C\left(h^{2k+2}\|\mathbf{u}\|_{2,k+1}^2+\sum_{i=r+1}^{d}\lambda_i\right) \tag{21}$$

$$\left\|\nabla\left(\mathbf{u}^n-\mathcal{P}_r\mathbf{u}^n\right)\right\|^2\le C\left(\left(h^{2k}+\|S_r\|_2 h^{2k+2}\right)\|\mathbf{u}\|_{2,k+1}^2+\zeta_r^2\right) \tag{22}$$

Now, we state the VMS-POD formulation of the NSE system. Find $\mathbf{u}_r\in\mathbf{X}_r$ satisfying:

$$\begin{aligned}&\left(\mathbf{u}_{r,t},\mathbf{v}_r\right)+\nu\left(\nabla\mathbf{u}_r,\nabla\mathbf{v}_r\right)+b\left(\mathbf{u}_r,\mathbf{u}_r,\mathbf{v}_r\right)\\&+\alpha\left(\left(I-\mathcal{P}_R\right)\nabla\mathbf{u}_r,\left(I-\mathcal{P}_R\right)\nabla\mathbf{v}_r\right)=\left(\mathbf{f},\mathbf{v}_r\right)\end{aligned} \tag{23}$$

for all $\mathbf{v}_r\in\mathbf{X}_r$. We equip (23) with the Crank-Nicholson temporal discretization (Eroglu & Kaya, 2020; Labovsky et al., 2009) and the VMS stabilization (Eroglu et al., 2019b; Iliescu & Wang, 2014). For simplicity, we use $\tilde{P}_R$ instead of $I-\mathcal{P}_R$. Let $\mathbf{f}\in L^2\left(0,\tau;\mathbf{H}^{-1}(\Omega)\right)$ and initial condition $\mathbf{u}_0\in\left(L^2(\Omega)\right)^d$ be given in $\mathbf{X}_r$. The extrapolated VMS-POD approximation for NSE (1) is given at time $t^n=n\Delta t$, $n=0,1,2,\ldots,M$ and $\tau=M\Delta t$, by:

$$\begin{aligned}&\left(\frac{\mathbf{u}_r^{n+1}-\mathbf{u}_r^n}{\Delta t},\mathbf{v}_r\right)+\nu\left(\nabla\mathbf{u}_r^{n/2},\nabla\mathbf{v}_r\right)+b\left(\mathcal{X}\left(\mathbf{u}_r^n\right),\mathbf{u}_r^{n/2},\mathbf{v}_r\right)\\&+\alpha\left(\tilde{P}_R\nabla\mathbf{u}_r^{n/2},\tilde{P}_R\nabla\mathbf{v}_r\right)=\left(\mathbf{f}\left(t^{n/2}\right),\mathbf{v}_r\right)\end{aligned} \tag{24}$$

where:

$$\mathcal{X}\left(\mathbf{u}_r^n\right)=\frac{3}{2}\mathbf{u}_r^n-\frac{1}{2}\mathbf{u}_r^{n-1},\mathbf{u}_r^{n/2}=\frac{\mathbf{u}_r^{n+1}+\mathbf{u}_r^n}{2} \tag{25}$$

and:

$$t^{n/2}=\frac{t^n+t^{n+1}}{2} \tag{26}$$

3. NUMERICAL ANALYSIS OF NSE

This section is devoted to a derivation of a priori error estimation of (24). We first give the stability of solution of (24).

Lemma 3.1. *(Stability) The scheme (24) is unconditionally stable in the following sense: for any* $\Delta t>0$:

$$\begin{aligned}&\left\|\mathbf{u}_r^{M+1}\right\|^2+\frac{\nu\Delta t}{2}\sum_{n=1}^{M}\left\|\nabla\mathbf{u}_r^{n/2}\right\|^2+\alpha\Delta t\sum_{n=1}^{M-1}\left\|\tilde{P}_R\nabla\mathbf{u}_r^{n/2}\right\|^2\\&\le\left\|\mathbf{u}_r^0\right\|^2+\nu^{-1}\|\mathbf{f}\|_{2,-1}^2\end{aligned} \tag{27}$$

Proof. Letting $\mathbf{v}_r=\mathbf{u}_r^{n/2}=\frac{\mathbf{u}_r^{n+1}+\mathbf{u}_r^n}{2}$ in (24) and using skew symmetry property yield:

$$\left(\frac{\mathbf{u}_r^{n+1}-\mathbf{u}_r^n}{\Delta t},\mathbf{u}_r^{n/2}\right)+\nu\left\|\nabla\mathbf{u}_r^{n/2}\right\|^2+\alpha\left\|\tilde{P}_R\nabla\mathbf{u}_r^{n/2}\right\|^2=\left(\mathbf{f}\left(t^{n/2}\right),\mathbf{u}_r^{n/2}\right) \tag{28}$$

Reorganizing the first term on the left hand side of (28), we get:

$$\frac{1}{\Delta t}\left\|\mathbf{u}_r^{n+1}\right\|^2-\frac{1}{\Delta t}\left\|\mathbf{u}_r^n\right\|^2+\nu\left\|\nabla\mathbf{u}_r^{n/2}\right\|^2+\alpha\left\|\tilde{P}_R\nabla\mathbf{u}_r^{n/2}\right\|^2=\left(\mathbf{f}\left(t^{n/2}\right),\mathbf{u}_r^{n/2}\right) \tag{29}$$

Applying the Cauchy-Schwarz, Young's inequalities on the right hand side of (29), and multiplying by Δt, produce:

$$\left\|\mathbf{u}_r^{n+1}\right\|^2-\left\|\mathbf{u}_r^n\right\|^2+\frac{\nu\Delta t}{2}\left\|\nabla\mathbf{u}_r^{n/2}\right\|^2+\alpha\Delta t\left\|\tilde{P}_R\nabla\mathbf{u}_r^{n/2}\right\|^2\le\nu^{-1}\Delta t\left\|\mathbf{f}\left(t^{n/2}\right)\right\|_{-1} \tag{30}$$

Summing from $n = 1$ to M gives the stated result (27).

The optimal asymptotic error estimation requires the following regularity assumptions for the true solution:

$$\begin{aligned}&\mathbf{u}\in L^\infty\left(0,k;\mathbf{H}^{k+1}(\Omega)\right)\\&\mathbf{u}_{tt}\in L^2\left(0,T;\mathbf{H}^1(\Omega)\right)\\&p\in L^\infty\left(0,k;H^k(\Omega)\right)\end{aligned} \tag{31}$$

Theorem 3.1. *(Error Estimation) Suppose regularity assumptions (31) hold. Then for the sufficiently small Δt, the error satisfies*:

$$\begin{aligned}\left\|\mathbf{u}^M-\mathbf{u}_r^M\right\|^2&\le K\Big(1+h^{2k}+(\Delta t)^4+\left(1+\left\|S_r\right\|_2+\left\|S_R\right\|_2\right)h^{2k+2}\\&+\sum_{i=r+1}^{d}\left(\left\|\xi_i\right\|_1^2+1\right)\lambda_i+\sum_{i=R+1}^{d}\left\|\xi_i\right\|_1^2\lambda_i\Big)\end{aligned} \tag{32}$$

Proof. We begin the proof by deriving error equation. By adding and subtracting some terms, continuous variational formulation (5) at time $\mathbf{v}_r=\mathbf{u}_r^{n/2}=\dfrac{\mathbf{u}_r^{n+1}+\mathbf{u}_r^n}{2}$ becomes:

$$\begin{aligned}&\left(\frac{\mathbf{u}\left(t^{n+1}\right)-\mathbf{u}\left(t^n\right)}{\Delta t},\mathbf{v}_r\right)+\nu\left(\nabla\mathbf{u}\left(t^{n/2}\right),\nabla\mathbf{v}_r\right)\\&+b\left(\mathbf{u}\left(t^{n/2}\right),\mathbf{u}\left(t^{n/2}\right),\mathbf{v}_r\right)-\left(p\left(t^{n/2}\right),\nabla\cdot\mathbf{v}_r\right)\\&+\alpha\left(\tilde{P}_R\nabla\mathbf{u}\left(t^{n/2}\right),\tilde{P}_R\nabla\mathbf{v}_r\right)\\&=\left(\mathbf{f}\left(t^{n/2}\right),\mathbf{v}_r\right)+\left(\frac{\mathbf{u}\left(t^{n+1}\right)-\mathbf{u}\left(t^n\right)}{\Delta t}-\mathbf{u}_t\left(t^{n/2}\right),\mathbf{v}_r\right)\\&+\alpha\left(\tilde{P}_R\nabla\mathbf{u}\left(t^{n/2}\right),\tilde{P}_R\nabla\mathbf{v}_r\right)\end{aligned} \tag{33}$$

Subtracting (24) from (33), we get:

$$\begin{aligned}&\left(\frac{\mathbf{u}\left(t^{n+1}\right)-\mathbf{u}\left(t^n\right)}{\Delta t}-\frac{\mathbf{u}_r^{n+1}-\mathbf{u}_r^n}{\Delta t},\mathbf{v}_r\right)+\nu\left(\nabla\left(\mathbf{u}\left(t^{n/2}\right)-\mathbf{u}_r^{n/2}\right),\nabla\mathbf{v}_r\right)\\&+b\left(\mathbf{u}\left(t^{n/2}\right),\mathbf{u}\left(t^{n/2}\right),\mathbf{v}_r\right)-b\left(\mathcal{X}\left(\mathbf{u}_r^n\right),\mathbf{u}_r^{n/2},\mathbf{v}_r\right)-\left(p\left(t^{n/2}\right),\nabla\cdot\mathbf{v}_r\right)\\&+\alpha\left(\tilde{P}_R\nabla\left(\mathbf{u}\left(t^{n/2}\right)-\mathbf{u}_r^{n/2}\right),\tilde{P}_R\nabla\mathbf{v}_r\right)=0\end{aligned} \tag{34}$$

The error term can be decomposed as:

$$\begin{aligned}\mathbf{u}\left(t^{n/2}\right)-\mathbf{u}_r^{n/2}&=\left(\mathbf{u}\left(t^{n/2}\right)-\mathbf{u}^{n/2}\right)-\left(\mathbf{u}_r^{n/2}-\mathbf{u}^{n/2}\right)\\&=\boldsymbol{\eta}^{n/2}-\phi_r^{n/2}\end{aligned} \tag{35}$$

where $\boldsymbol{\eta}^{n/2}=\mathbf{u}^{n/2}-\tilde{\mathbf{u}}^{n/2},\phi_r^{n/2}=\mathbf{u}_r^{n/2}-\tilde{\mathbf{u}}^{n/2}$, and $\tilde{\mathbf{u}}^{n/2}$ is L^2 projections of $\mathbf{u}^{n/2}$ in $\mathbf{X}_r$ at time $t^{n/2}$:

Adding and subtracting the terms:

$$\begin{aligned}&\pm b\left(\mathbf{u}_r^{n/2},\mathbf{u}\left(t^{n/2}\right),\mathbf{v}_r\right),\pm b\left(\mathbf{u}_r^{n/2},\mathbf{u}_r^{n/2},\mathbf{v}_r\right),\pm b\left(\mathbf{u}\left(t^{n/2}\right),\mathbf{u}_r^{n/2},\mathbf{v}_r\right),\\&\pm b\left(\mathbf{u}\left(t^n\right),\mathbf{u}_r^{n/2},\mathbf{v}_r\right),\pm b\left(\mathcal{X}\left(\mathbf{u}\left(t^n\right)\right),\mathbf{u}_r^{n/2},\mathbf{v}_r\right)\end{aligned}$$

the nonlinear terms become:

$$\begin{aligned}&b\left(\mathbf{u}\left(t^{n/2}\right),\mathbf{u}\left(t^{n/2}\right),\mathbf{v}_r\right)-b\left(\mathcal{X}\left(\mathbf{u}_r^n\right),\mathbf{u}_r^{n/2},\mathbf{v}_r\right)\\&=b\left(\boldsymbol{\eta}^{n/2},\mathbf{u}\left(t^{n/2}\right),\mathbf{v}_r\right)-b\left(\phi_r^{n/2},\mathbf{u}\left(t^{n/2}\right),\mathbf{v}_r\right)+b\left(\mathbf{u}_r^{n/2},\boldsymbol{\eta}^{n/2},\mathbf{v}_r\right)\\&-b\left(\mathbf{u}_r^{n/2},\phi_r^{n/2},\mathbf{v}_r\right)-b\left(\boldsymbol{\eta}^{n/2},\mathbf{u}_r^{n/2},\mathbf{v}_r\right)+b\left(\phi_r^{n/2},\mathbf{u}_r^{n/2},\mathbf{v}_r\right)\\&+b\left(\mathbf{u}\left(t^{n/2}\right)-\mathbf{u}\left(t^n\right),\mathbf{u}_r^{n/2},\mathbf{v}_r\right)+b\left(\mathbf{u}\left(t^n\right)-\mathcal{X}\left(\mathbf{u}\left(t^n\right)\right),\mathbf{u}_r^{n/2},\mathbf{v}_r\right)\\&+b\left(\mathcal{X}\left(\boldsymbol{\eta}^n\right),\mathbf{u}_r^{n/2},\mathbf{v}_r\right)-b\left(\mathcal{X}\left(\phi_r^n\right),\mathbf{u}_r^{n/2},\mathbf{v}_r\right)\end{aligned} \tag{36}$$

Inserting (35) and (35) in (34), letting $\mathbf{v}_r=\phi_r^{n/2}$ and using $b\left(\mathbf{u}_r^{n/2},\phi_r^{n/2},\phi_r^{n/2}\right)=0$, we have:

$$\begin{aligned}&\left(\frac{\phi_r^{n+1}-\phi_r^n}{\Delta t},\phi_r^{n/2}\right)+\nu\left\|\nabla\phi_r^{n/2}\right\|^2+\alpha\left\|\tilde{P}_R\nabla\phi_r^{n/2}\right\|^2\\&=\left(\frac{\eta^{n+1}-\eta^n}{\Delta t},\phi_r^{n/2}\right)+\nu\left(\nabla\eta^{n/2},\nabla\phi_r^{n/2}\right)-\left(p\left(t^{n/2}\right),\nabla\cdot\phi_r^{n/2}\right)\\&+b\left(\boldsymbol{\eta}^{n/2},\mathbf{u}\left(t^{n/2}\right),\phi_r^{n/2}\right)-b\left(\phi_r^{n/2},\mathbf{u}\left(t^{n/2}\right),\phi_r^{n/2}\right)\\&+b\left(\mathbf{u}_r^{n/2},\boldsymbol{\eta}^{n/2},\phi_r^{n/2}\right)-b\left(\boldsymbol{\eta}^{n/2},\mathbf{u}_r^{n/2},\phi_r^{n/2}\right)+b\left(\phi_r^{n/2},\mathbf{u}_r^{n/2},\phi_r^{n/2}\right)\\&+b\left(\mathbf{u}\left(t^{n/2}\right)-\mathbf{u}\left(t^n\right),\mathbf{u}_r^{n/2},\phi_r^{n/2}\right)+b\left(\mathbf{u}\left(t^n\right)-\mathcal{X}\left(\mathbf{u}\left(t^n\right)\right),\mathbf{u}_r^{n/2},\phi_r^{n/2}\right)\\&+b\left(\mathcal{X}\left(\boldsymbol{\eta}^n\right),\mathbf{u}_r^{n/2},\phi_r^{n/2}\right)-b\left(\mathcal{X}\left(\phi_r^n\right),\mathbf{u}_r^{n/2},\phi_r^{n/2}\right)\\&+\alpha\left(\tilde{P}_R\nabla\eta^{n/2},\tilde{P}_R\nabla\phi_r^{n/2}\right)+\left(\mathbf{u}_t^{n+1}-\frac{\mathbf{u}^{n+1}-\mathbf{u}^n}{\Delta t},\phi_r^{n+1}\right)\end{aligned} \tag{37}$$

Reorganizing (37), we get:

$$\begin{aligned}
&\frac{1}{\Delta t}\left\|\phi_r^{n+1}\right\|^2-\frac{1}{\Delta t}\left\|\phi_r^{n}\right\|^2+\nu\left\|\nabla\phi_r^{n/2}\right\|^2+\alpha\left\|\tilde{P}_R\nabla\phi_r^{n/2}\right\|^2\\
&\le\left|\left(\frac{\boldsymbol{\eta}^{n+1}-\boldsymbol{\eta}^{n}}{\Delta t},\phi_r^{n/2}\right)\right|+\nu\left|\left(\nabla\boldsymbol{\eta}^{n/2},\nabla\phi_r^{n/2}\right)\right|+\left|\left(p\left(t^{n/2}\right)-q_h,\nabla\cdot\phi_r^{n/2}\right)\right|\\
&+\left|b\left(\boldsymbol{\eta}^{n/2},\mathbf{u}\left(t^{n/2}\right),\phi_r^{n/2}\right)\right|+\left|b\left(\phi_r^{n/2},\mathbf{u}\left(t^{n/2}\right),\phi_r^{n/2}\right)\right|+\left|b\left(\mathbf{u}_r^{n/2},\boldsymbol{\eta}^{n/2},\phi_r^{n/2}\right)\right|\\
&+\left|b\left(\boldsymbol{\eta}^{n/2},\mathbf{u}_r^{n/2},\phi_r^{n/2}\right)\right|+\left|b\left(\phi_r^{n/2},\mathbf{u}_r^{n/2},\phi_r^{n/2}\right)\right|\\
&+\left|b\left(\mathbf{u}\left(t^{n/2}\right)-\mathbf{u}\left(t^{n}\right),\mathbf{u}_r^{n/2},\phi_r^{n/2}\right)\right|+\left|b\left(\mathbf{u}\left(t^{n}\right)-\mathcal{X}\left(\mathbf{u}\left(t^{n}\right)\right),\mathbf{u}_r^{n/2},\phi_r^{n/2}\right)\right|\\
&+\left|b\left(\mathcal{X}\left(\boldsymbol{\eta}^{n}\right),\mathbf{u}_r^{n/2},\phi_r^{n/2}\right)\right|+\left|b\left(\mathcal{X}\left(\phi_r^{n}\right),\mathbf{u}_r^{n/2},\phi_r^{n/2}\right)\right|\\
&+\alpha\left|\left(\tilde{P}_R\nabla\boldsymbol{\eta}^{n/2},\tilde{P}_R\nabla\phi_r^{n/2}\right)\right|+\left|\left(\mathbf{u}_t^{n+1}-\frac{\mathbf{u}^{n+1}-\mathbf{u}^{n}}{\Delta t},\phi_r^{n/2}\right)\right|
\end{aligned}\tag{38}$$

The first term on the right hand side of (38) vanishes by using (17). The other terms can be bounded by using Cauchy-Schwarz and Young's inequalities as:

$$\begin{aligned}
&\nu\left|\left(\nabla\boldsymbol{\eta}^{n/2},\nabla\phi_r^{n/2}\right)\right|\le K\nu\left\|\nabla\boldsymbol{\eta}^{n/2}\right\|^2+\frac{\nu}{20}\left\|\nabla\phi_r^{n/2}\right\|^2\\
&\left|\left(p\left(t^{n/2}\right)-q_h,\nabla\cdot\phi_r^{n/2}\right)\right|\le K\nu^{-1}\left\|p^{n+1}-q_h\right\|^2+\frac{\nu}{20}\left\|\nabla\phi_r^{n/2}\right\|^2\\
&\alpha\left|\left(\tilde{P}_R\nabla\boldsymbol{\eta}^{n/2},\tilde{P}_R\nabla\phi_r^{n/2}\right)\right|\le\frac{\alpha}{2}\left\|\tilde{P}_R\nabla\boldsymbol{\eta}^{n/2}\right\|^2+\frac{\alpha}{2}\left\|\tilde{P}_R\nabla\phi_r^{n/2}\right\|^2\\
&\left|\left(\mathbf{u}_t^{n+1}-\frac{\mathbf{u}^{n+1}-\mathbf{u}^{n}}{\Delta t},\phi_r^{n/2}\right)\right|\le K\nu^{-1}\left\|\mathbf{u}_t^{n+1}-\frac{\mathbf{u}^{n+1}-\mathbf{u}^{n}}{\Delta t}\right\|^2+\frac{\nu}{20}\left\|\nabla\phi_r^{n/2}\right\|^2
\end{aligned}\tag{39}$$

The nonlinear terms are bounded as:

$$\begin{aligned}
&\left|b\left(\boldsymbol{\eta}^{n/2},\mathbf{u}\left(t^{n/2}\right),\phi_r^{n/2}\right)\right|\le K\nu^{-1}\left\|\nabla\boldsymbol{\eta}^{n/2}\right\|^2\left\|\nabla\mathbf{u}\left(t^{n/2}\right)\right\|^2+\frac{\nu}{20}\left\|\nabla\phi_r^{n/2}\right\|^2,\\
&\left|b\left(\phi_r^{n/2},\mathbf{u}\left(t^{n/2}\right),\phi_r^{n/2}\right)\right|+\left|b\left(\phi_r^{n/2},\mathbf{u}_r^{n/2},\phi_r^{n/2}\right)\right|\le K\nu^{-3}\left\|\phi_r^{n/2}\right\|^2\left(\left\|\nabla\mathbf{u}\left(t^{n/2}\right)\right\|^4+\left\|\nabla\mathbf{u}_r^{n/2}\right\|^4\right)+\frac{\nu}{20}\left\|\nabla\phi_r^{n/2}\right\|^2\\
&\left|b\left(\mathbf{u}_r^{n/2},\boldsymbol{\eta}^{n/2},\phi_r^{n/2}\right)\right|+\left|b\left(\boldsymbol{\eta}^{n/2},\mathbf{u}_r^{n/2},\phi_r^{n/2}\right)\right|\le K\nu^{-1}\left\|\nabla\mathbf{u}_r^{n/2}\right\|^2\left\|\nabla\boldsymbol{\eta}^{n/2}\right\|^2+\frac{\nu}{20}\left\|\nabla\phi_r^{n/2}\right\|^2\\
&\left|b\left(\mathbf{u}\left(t^{n/2}\right)-\mathbf{u}\left(t^{n}\right),\mathbf{u}_r^{n/2},\phi_r^{n/2}\right)\right|\le K\nu^{-1}\left\|\nabla\left(\mathbf{u}\left(t^{n/2}\right)-\mathbf{u}\left(t^{n}\right)\right)\right\|\left\|\nabla\mathbf{u}_r^{n/2}\right\|^2+\frac{\nu}{20}\left\|\nabla\phi_r^{n/2}\right\|^2\\
&\left|b\left(\mathbf{u}\left(t^{n}\right)-\mathcal{X}\left(\mathbf{u}\left(t^{n}\right)\right),\mathbf{u}_r^{n/2},\phi_r^{n/2}\right)\right|\le K\nu^{-1}\left\|\nabla\left(\mathbf{u}\left(t^{n}\right)-\mathcal{X}\left(\mathbf{u}\left(t^{n}\right)\right)\right)\right\|\left\|\nabla\mathbf{u}_r^{n/2}\right\|^2+\frac{\nu}{20}\left\|\nabla\phi_r^{n/2}\right\|^2\\
&\left|b\left(\mathcal{X}\left(\boldsymbol{\eta}^{n}\right),\mathbf{u}_r^{n/2},\phi_r^{n/2}\right)\right|\le K\nu^{-1}\left\|\nabla\mathcal{X}\left(\boldsymbol{\eta}^{n}\right)\right\|\left\|\nabla\mathbf{u}_r^{n/2}\right\|^2+\frac{\nu}{20}\left\|\nabla\phi_r^{n/2}\right\|^2\\
&\left|b\left(\mathcal{X}\left(\phi_r^{n}\right),\mathbf{u}_r^{n/2},\phi_r^{n/2}\right)\right|\le K\nu^{-1}\left\|\nabla\mathcal{X}\left(\phi_r^{n}\right)\right\|\left\|\nabla\mathbf{u}_r^{n/2}\right\|2+\frac{\nu}{20}\left\|\nabla\phi_r^{n/2}\right\|^2
\end{aligned}\tag{40}$$

Substituting all bounds into (38) yields:

$$\begin{aligned}
&\frac{1}{\Delta t}\left\|\phi_r^{n+1}\right\|^2-\frac{1}{\Delta t}\left\|\phi_r^{n}\right\|^2+\frac{\nu}{2}\left\|\nabla\phi_r^{n/2}\right\|^2+\frac{\alpha}{2}\left\|\tilde{P}_R\nabla\phi_r^{n/2}\right\|^2\le K\Bigg(\nu\left\|\nabla\boldsymbol{\eta}^{n/2}\right\|^2+\nu^{-1}\left\|\nabla\boldsymbol{\eta}^{n/2}\right\|^2\left\|\nabla\mathbf{u}\left(t^{n/2}\right)\right\|^2+\nu^{-3}\left\|\phi_r^{n/2}\right\|^2\left(\left\|\nabla\mathbf{u}\left(t^{n/2}\right)\right\|^4+\left\|\nabla\mathbf{u}_r^{n/2}\right\|^4\right)\\
&+\frac{\alpha}{2}\left\|\tilde{P}_R\nabla\boldsymbol{\eta}^{n/2}\right\|^2+\nu^{-1}\left\|\nabla\mathbf{u}_r^{n/2}\right\|^2\left\|\nabla\boldsymbol{\eta}^{n/2}\right\|^2+\nu^{-1}\left\|\nabla\left(\mathbf{u}\left(t^{n/2}\right)-\mathbf{u}\left(t^{n}\right)\right)\right\|\left\|\nabla\mathbf{u}_r^{n/2}\right\|^2+\nu^{-1}\left\|\nabla\left(\mathbf{u}\left(t^{n}\right)-\mathcal{X}\left(\mathbf{u}\left(t^{n}\right)\right)\right)\right\|\left\|\nabla\mathbf{u}_r^{n/2}\right\|^2+\nu^{-1}\left\|\nabla\mathcal{X}\left(\boldsymbol{\eta}^{n}\right)\right\|\left\|\nabla\mathbf{u}_r^{n/2}\right\|^2\\
&+\nu^{-1}\left\|\nabla\mathcal{X}\left(\phi_r^{n}\right)\right\|\left\|\nabla\mathbf{u}_r^{n/2}\right\|^2+\left\|p\left(t^{n/2}\right)-q_h\right\|^2+\left\|\mathbf{u}_t^{n+1}-\frac{\mathbf{u}^{n+1}-\mathbf{u}^{n}}{\Delta t}\right\|^2\Bigg)
\end{aligned}\tag{41}$$

We now multiply (41) by $2\Delta t$, sum over the time steps and use Lemma 3.1 to get:

$$\begin{aligned}
&\left\|\phi_r^{M}\right\|^2+\nu\Delta t\sum_{n=1}^{M-1}\left\|\nabla\phi_r^{n/2}\right\|^2+\alpha\Delta t\sum_{n=1}^{M-1}\left\|\tilde{P}_R\nabla\phi_r^{n/2}\right\|^2\\
&\le\left\|\phi_r^{0}\right\|^2+K\Delta t\left(\sum_{n=1}^{M-1}\left(\nu+\nu^{-1}\left\|\nabla\mathbf{u}\left(t^{n/2}\right)\right\|^2+\nu^{-1}\left\|\nabla\mathbf{u}_r^{n/2}\right\|^2\right)\left\|\nabla\boldsymbol{\eta}^{n/2}\right\|^2\right.\\
&+\alpha\sum_{n=1}^{M-1}\left\|\tilde{P}_R\nabla\boldsymbol{\eta}^{n/2}\right\|^2+\nu^{-1}\sum_{n=1}^{M-1}\left(\left\|\nabla\left(\mathbf{u}\left(t^{n/2}\right)-\mathbf{u}\left(t^{n}\right)\right)\right\|^2+\nu^{-1}\left\|\nabla\left(\mathbf{u}\left(t^{n}\right)-\mathcal{X}\left(\mathbf{u}\left(t^{n}\right)\right)\right)\right\|^2+\nu^{-1}\left\|\nabla\mathcal{X}\left(\boldsymbol{\eta}^{n}\right)\right\|^2\right)\left\|\nabla\mathbf{u}_r^{n/2}\right\|^2\\
&\left.+\sum_{n=1}^{M-1}\left\|p\left(t^{n/2}\right)-q_h\right\|^2+\sum_{n=1}^{M-1}\left\|\mathbf{u}_t^{n+1}-\frac{\mathbf{u}^{n+1}-\mathbf{u}^{n}}{\Delta t}\right\|^2\right)+\nu^{-1}h^{-2}\left(\left\|\mathbf{u}_r^{0}\right\|^2+\nu^{-1}\|\mathbf{f}\|_{2,-1}^2\right)\Delta t\sum_{n=1}^{M-1}\left(\frac{9}{4}\left\|\phi_r^{n}\right\|^2+\frac{1}{4}\left\|\phi_r^{n-1}\right\|^2\right)\\
&+\nu^{-3}\left(\left\|\nabla\mathbf{u}\right\|_{\infty,0}^2+\left\|\mathbf{u}_r^{0}\right\|^2+\nu^{-1}\|f\|_{2,-1}^2\right)\Delta t\sum_{n=1}^{M-1}\left(\frac{1}{4}\left\|\phi_r^{n}\right\|^2+\frac{1}{4}\left\|\phi_r^{n+1}\right\|^2\right)
\end{aligned}\tag{42}$$

To simplify the last two terms on the right hand side of (42), we define:

$$S^{n+1} = \begin{cases} 2\nu^{-3}|||\nabla \mathbf{u}|||^2_{\infty,0} + \left(2\nu^{-3} + 2\nu^{-1}h^{-2}\right)\left(\|\mathbf{u}_r^0\|^2 + \nu^{-1}\|\mathbf{f}\|^2_{2,-1}\right) & if\ 1 \le n \le M-3 \\ 2\nu^{-3}|||\nabla \mathbf{u}|||^2_{\infty,0} + \left(2\nu^{-3} + \nu^{-1}h^{-2}\right)\left(\|\mathbf{u}_r^0\|^2 + \nu^{-1}\|\mathbf{f}\|^2_{2,-1}\right) & if\ n = M-2 \\ \nu^{-3}|||\nabla \mathbf{u}|||^2_{\infty,0} + \|\mathbf{u}_r^0\|^2 + \nu^{-1}|||\mathbf{f}|||^2_{2,-1} & if\ n = M-1 \end{cases} \tag{43}$$

Substituting (43), the equation (42) becomes:

$$\begin{aligned} &\|\phi_r^M\|^2 + \nu\Delta t\sum_{n=1}^{M-1}\|\nabla\phi_r^{n/2}\|^2 + \alpha\Delta t\sum_{n=1}^{M-1}\|\tilde{P}_R\nabla\phi_r^{n/2}\|^2 \le \|\phi_r^0\|^2 + K\Delta t\Bigg(\sum_{n=1}^{M-1}\left(\nu + \nu^{-1}\|\nabla\mathbf{u}(t^{n/2})\|^2 + \nu^{-1}\|\nabla\mathbf{u}_r^{n/2}\|^2\right)\|\nabla\boldsymbol{\eta}^{n/2}\|^2 \\ &+\alpha\sum_{n=1}^{M-1}\|\tilde{P}_R\nabla\boldsymbol{\eta}^{n/2}\|^2 + \nu^{-1}\sum_{n=1}^{M-1}\left(\|\nabla(\mathbf{u}(t^{n/2}) - \mathbf{u}(t^n))\|^2 + \nu^{-1}\|\nabla(\mathbf{u}(t^n) - \mathcal{X}(\mathbf{u}(t^n)))\|^2\right. \\ &\left.+\nu^{-1}\|\nabla\mathcal{X}(\boldsymbol{\eta}^n)\|^2\right)\|\nabla\mathbf{u}_r^{n/2}\|^2 + \sum_{n=1}^{M-1}\|p(t^{n/2}) - q_h\|^2 + \sum_{n=1}^{M-1}\left\|\mathbf{u}_t^{n+1} - \frac{\mathbf{u}^{n+1}-\mathbf{u}^n}{\Delta t}\right\|^2\Bigg) + \Delta t\sum_{n=1}^{M-1}S^{n+1}\|\phi_r^{n+1}\|^2 \end{aligned} \tag{44}$$

The term $\nu^{-1}\sum_{n=1}^{M-1}\|\nabla(\mathbf{u}(t^{n/2}) - \mathbf{u}(t^n))\|^2\|\nabla\mathbf{u}_r^{n/2}\|^2$ is bounded by using the standard a priori error estimate on the true solution, regularity assumptions (31) and Lemma 3.1. In a similar manner, the terms on the right hand side of (44) can be bounded as:

$$\begin{aligned} &\Delta t\sum_{n=1}^{M-1}\left(\nu + \nu^{-1}\|\nabla\mathbf{u}(t^{n/2})\|^2 + \nu^{-1}\|\nabla\mathbf{u}_r^{n/2}\|^2\right)\|\nabla\boldsymbol{\eta}^{n/2}\|^2 \\ &\le K\left(\left(h^{2k} + \|S_r\|_2 h^{2k+2}\right)|||\mathbf{u}|||^2_{2,k+1} + \zeta_r^2\right) \end{aligned} \tag{45}$$

$$\alpha\sum_{n=1}^{M-1}\|\tilde{P}_R\nabla\boldsymbol{\eta}^{n/2}\|^2 \le K\left(\left(h^{2k} + \|S_R\|_2 h^{2k+2}\right)|||\mathbf{u}|||^2_{2,k+1} + \zeta_R^2\right) \tag{46}$$

$$\nu^{-1}\sum_{n=1}^{M-1}\|\nabla(\mathbf{u}(t^n) - \mathcal{X}(\mathbf{u}(t^n)))\|^2\|\nabla\mathbf{u}_r^{n/2}\|^2 \le K\nu^{-1}\Delta t^4\|\mathbf{u}_{tt}\|^2_{L^2(0,T;L^2(\Omega))} \tag{47}$$

$$\begin{aligned} &\nu^{-1}\sum_{n=1}^{M-1}\|\nabla\mathcal{X}(\boldsymbol{\eta}^n)\|^2\|\nabla\mathbf{u}_r^{n/2}\|^2 \\ &\le K\nu^{-1}\left(\left(h^{2k} + \|S_r\|_2 h^{2k+2}\right)|||\mathcal{X}(\mathbf{u})|||^2_{2,k+1} + \zeta_r^2\right) \end{aligned} \tag{48}$$

$$\nu^{-1}\Delta t\sum_{n=1}^{M-1}\|p(t^{n/2}) - q_h\|^2 \le K\nu^{-1}h^{2k}|||p|||^2_{2,k} \tag{49}$$

$$\nu^{-1}\Delta t\sum_{n=1}^{M-1}\left\|\mathbf{u}_t^{n+1} - \frac{\mathbf{u}^{n+1}-\mathbf{u}^n}{\Delta t}\right\|^2 \le K\nu^{-1}(\Delta t)^2\|\mathbf{u}_{tt}\|^2_{L^2(0,T;H^1(\Omega))}, \tag{50}$$

where:

$$\zeta_r = \sqrt{\sum_{i=r+1}^{d}\|\xi_i\|_1^2\lambda_i}, \quad \zeta_R = \sqrt{\sum_{i=R+1}^{d}\|\xi_i\|_1^2\lambda_i} \tag{51}$$

Inserting all bounds in (44), using (21), Lemma 2.1, Lemma 3.1 and applying regularity assumptions (31) lead to:

$$\begin{aligned} &\|\phi_r^M\|^2 + \Delta t\sum_{n=1}^{M-1}\nu\|\nabla\phi_r^{n/2}\|^2 \le \|\mathbf{u}_r^0 - \mathbf{u}^0\|^2 \\ &+K\Big(h^{2k} + \Delta t^4 + \left(1 + \|S_r\|_2 + \|S_R\|_2\right)h^{2k+2} \\ &+\zeta_r^2 + \zeta_R^2 + \Delta t\sum_{n=1}^{M-1}S^{n+1}\|\phi_r^{n+1}\|^2\Big) \end{aligned} \tag{52}$$

Applying the discrete Gronwall inequality for $\Delta t \le 1/S^{n+1}$, using the assumption $\mathbf{u}_r^0 = \tilde{\mathbf{u}}^0$, the triangle inequality and (21) yields the stated result.

4. NUMERICAL STUDIES

This section presents the results of two numerical tests. In the first test, we calculated the convergence rates of the method with respect to R. In the second test, we compared the accuracy of the proposed extrapolated VMS-POD method with the standard VMS-POD method. Direct numerical solution (DNS) has been computed by using standard Galerkin FEM discretization. We use the benchmark problem of 2D channel flow around a circular cylinder presented in figure 1, see (Schäffer & Turek, 1996; John, 2004).

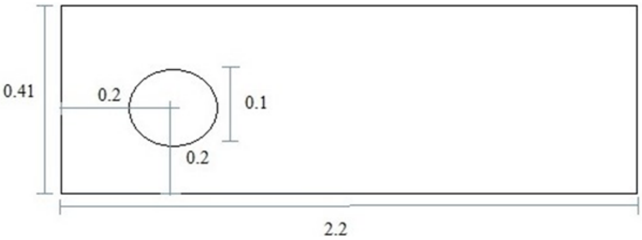

Fig. 1. *2D channel flow past a circular cylinder domain.*

For the walls and cylinder, the test problem satisfies the no-slip boundary conditions and the inflow and outflow conditions are prescribed by:

$$u_1(0,y,t) = u_1(2.2,y,t) = \frac{6y(0.41-y)}{0.41^2} \qquad (53)$$
$$u_2(0,y,t) = u_2(2.2,y,t) = 0$$

4.1. Test 1: Convergence rates wrt R

To verify the numerical analysis of (24) with respect to R, we fix $r = 10$, $\Delta t = 0{:}02$, $T = 3$, $\nu = 0{:}001$, $\alpha = 0{:}0003$. The VMS contribution to the error is defined by ζR in (51). Errors and convergence rates are listed in table 1 for increasing values of R. We note that the rates of convergence are nearly 0:5 or higher than predicted by theoretical analysis:

4.2. Test 1: Accuracy of the extrapolated VMS-POD method

In this test, we compared the accuracy of extrapolated VMS-POD with the VMS-POD method. Figure 2 shows that the proposed extrapolation increase the efficiency of VMS-POD method. We observe that the extrapolated scheme gives better result than unextrapolated scheme for $R = 2$. Moreover, the extrapolated VMS-POD solution matches exactly the DNS solution for $R = 4$.

Table 1*. Convergence of the extrapolated VMS-POD for r = 10 and varying R.*

R	ζ_R	$\left\lVert \mathbf{u}^M - \mathbf{u}_r^M \right\rVert L^2\left(L^\infty(\Omega)\right)$	rate	$\left\lVert \mathbf{u}^M - \mathbf{u}_r^M \right\rVert L^2\left(H^1(\Omega)\right)$	rate
4	13.4579	0.064273779027008	-	4.799267941923246	-
5	5.4549	0.042544931339859	0.46	3.074404809792470	0.49
6	3.4015	0.028581358335344	0.84	1.874130691309018	1.04

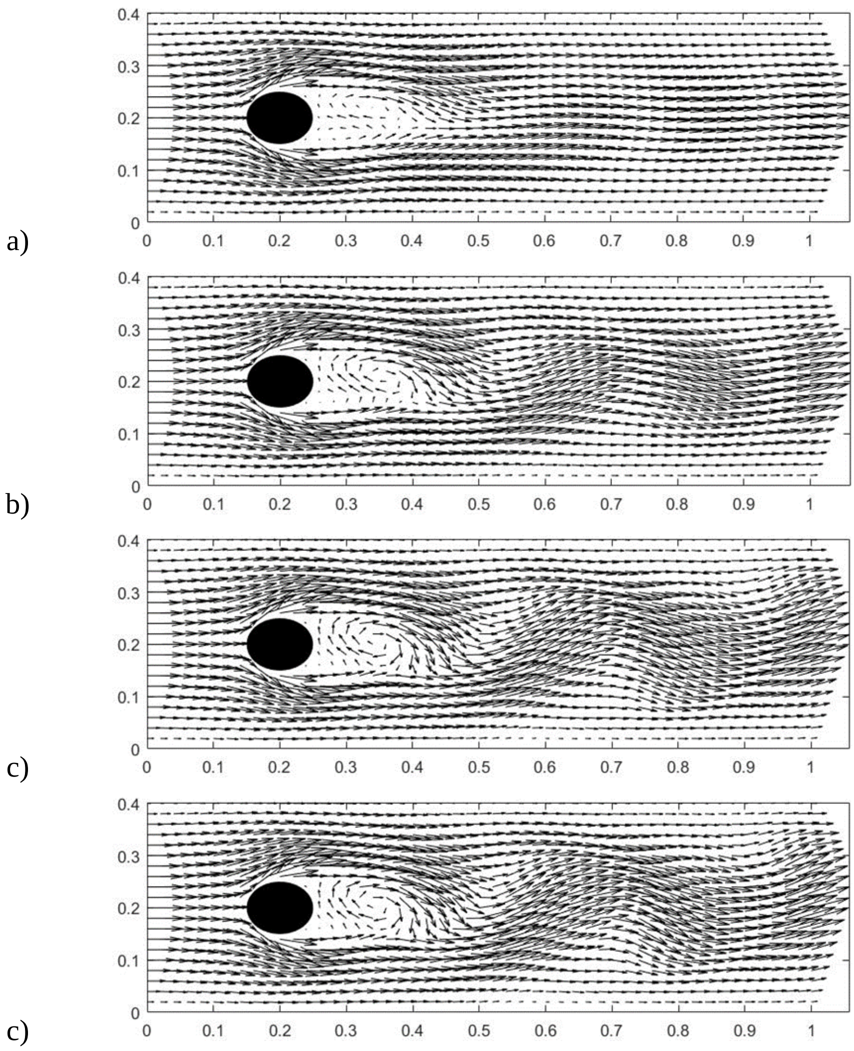

Fig. 2. *Solution plots for the simulations using VMS-POD (R = 2) (a), Extrapolated VMS-POD (R = 2) (b), Extrapolated VMS-POD (R = 4) (c) and DNS (d).*

5. CONCLUSIONS

We presented an extrapolated VMS-POD method for the NSE. The stability and convergence analyses for the scheme are proved. We examined convergence rates with respect to R. The results of the numerical test on the benchmark problem confirm the theoretical findings. We also compared the accuracy of the extrapolated VMS-POD method with standard VMS-POD method. Results of numerical experiments indicate that the addition of extrapolation improves the accuracy of the VMS-POD method.

REFERENCES

Eroglu, F., Kaya, S., Rebholz, L., 2017, A modular regularized variational multiscale proper orthogonal decomposition for incompressible flows, *Comput. Methods Appl. Mech. Engrg.*, 325, 350-368.

Eroglu, F., Kaya, S., Rebholz, L., 2019a, POD-ROM for the Darcy-Brinkman equations with double-diffusive convection, *J. Numer. Math*. , 27(3), 123-139.

Eroglu, F., Kaya, S., Rebholz, L., 2019b, Decoupled Modular Regularized VMS-POD for DarcyBrinkman Equations, *IAENG International Journal of Applied Mathematics*, 49(2), 134-144.

Eroglu, F., Kaya, S., 2020, An extrapolated Crank Nicholson VMS-POD method for Darcy Brinkman equations, *Numerical Solutions of Realistic Nonlinear Phenomena*, eds, Machado, J.A.T., Ozdemir, N., Baleanu, D., Springer (in press).

Iliescu, T., Wang, Z., 2013, Variational multiscale proper orthogonal decomposition: convectiondominated convection-diffusion-reaction equations, *Mathematics of Computation*, 82(283), 1357-1378.

Iliescu T., Wang Z., 2014, Variational multiscale proper orthogonal decomposition: Navier-Stokes Equations, *Numer. Meth. Partial. Diff. Eqs*., 30(2), 641-663.

John, V., 2004, Reference values for drag and lift of a two-dimensional time-dependent flow around a cylinder, *Int. J. Numer. Meth. Fluids*, 44, 777-788.

John, V., Kaya, S., Layton, W., 2006, A two-level variational multiscale method for convectiondominated convection-diffusion equations, *Comput. Methods Appl. Mech. Engrg*., 195, 4594-4603.

John, V., Kaya, S., 2008, Finite element error analysis of a variational multiscale method for the Navier-Stokes equations, *Adv. Comput. Math*., 28, 43-61.

Kalugin, M.D., Strijhak, S.V., 2016, Implementation of POD and DMD methods in apache spark framework for simulation of unsteady turbulent flow in the model combustor, *Proc. Conf. ECCOMAS 2016*, eds, Papadrakakis, M., Papadopoulos, V., Stefanou G., Plevris, V., Crete Island, 857-864.

Kunisch, K., Volkwein, S., 2001, Galerkin proper orthogonal decomposition methods for parabolic problems, *Numerische Mathematik*, 90(1), 117-148.

Labovsky, A., Layton, W., Manica, C., Neda, M., Rebholz, L., 2009, The stabilized extrapolated trapezoidal finite-element method for the Navier-Stokes equations, *Comput. Methods Appl. Mech. Engrg*., 198, 958-974.

Roop, J.P., 2013, A Proper-Orthogonal decomposition variational multiscale approximation method for a generalized Oseen problem, *Advances in Numerical Analysis*, 2013, 1-8.

San, O., Borggaard, J., 2015, Principal interval decomposition framework for POD reducedorder modeling of convective Boussinesq flows, *Int. J. Numer. Meth. Fluids*, 78, 37-62.

Schäfer, M., Turek, S., 1996, Benchmark computations of laminar flow around a cylinder (with support by Durst, F., Krause, E. and Rannacher, R.), Flow Simulation with High-Performance Computers II. *Notes on Numerical Fluid Mechanics (NNFM)*, ed., Hirschel, E.H., Vieweg, Wiesbaden, 547-566.

Xia, L., Raghavan, B., Breitkopf, P., Zhang, W., 2013, A POD/PGD reduction approach for an efficient parameterization of data-driven material microstructure models, *Computer Methods in Materials Science*, 13, 219-225.

EKSTRAPOLACYJNA METODA VMS-POD DLA NIEŚCIŚLLIWYCH PRZEPŁYWÓW

Streszczenie

W artykule zastosowano obniżenie rzędu modelu i wariacyjną wieloskalową stabilizację, wykorzystujące ortogonalną dekompozycję, do rozwiązania równania Naviera-Stokesa dla nieściśliwych płynów. Trudności wynikające z nieliniowości wyeliminowano poprzez zastosowanie ekstrapolacji. W pracy opisano teoretyczne podstawy metody. W celu sprawdzenia wydajności opracowanej metody zastosowano ję do testowego problemu przepływu 2D przez cylindryczny kanał.

Received: August 27, 2019.
Received in a revised form: November 14, 2019.
Accepted: December 4, 2019.